

## SPACEBORNE ELECTRON ACCELERATORS\*

J.W. Lewellen<sup>†</sup>, C. Buechler, G. Dale, N.A. Moody, D.C. Nguyen  
Los Alamos National Laboratory, Los Alamos, United States

### Abstract

High-power electron beam generators in space will enable the studies of solar and space physics, specifically the interrogation of the magnetic connection between the magnetosphere and ionosphere. The CONNEX collaboration plans to map the magnetic connection between the magnetosphere and ionosphere, using a satellite equipped with an electron beam accelerator that can create a spot in the ionosphere – an artificial aurora – observable by optical and radar detectors on the ground.

To date, a number of spacecraft carrying low-power, <50 keV DC electron beam sources have been launched to study the upper ionosphere, however, reaching the average beam power required for future missions requires a switch to RF technology. We present the concept for a quasi-CW, C-band electron accelerator with 1-MeV beam energy, 10-mA beam current, and requiring 40 kW of prime power during operation. Our novel accelerator concept includes the following features: individually powered cavities driven by 5 GHz high-electron mobility transistors (HEMT), passively cooled accelerator structures, and active frequency control for operating over a range of temperatures.

### INTRODUCTION

The earth's magnetosphere is the region surrounding the earth in which its magnetic field is the dominant influence on charged-particle dynamics. Near the surface, it can be approximated by a dipole field, but further out it becomes an increasingly structurally complex and time-varying phenomenon, as it is influenced by the solar wind as well as geodynamics. Existing models of the magnetosphere are mostly empirical, and measurements are obtained primarily by magnetometer data from spacecraft [1,2]. These provide the magnetic field at a particular location but little direct data elsewhere.

The CONNEX collaboration proposes using an electron beam to probe the coupling between the magnetosphere and ionosphere. The intent is to direct an electron beam into the “loss cone” [3], approximately parallel to the earth's field at the satellite's location, which will result in the beam being lost in the ionosphere. As the beam enters the atmosphere it generates ionization and auroral glow, which can be observed via ground-based camera and radar observation. Thus, knowing the location of the satellite and the beam's re-entry point, we obtain information about the

magnetic connection between the satellite's location and the ionosphere.

The intensity of the optical signature depends more strongly on the total beam power and net energy deposited than on the beam voltage. Approximately 10 kJ – 1 kW average power over 10 s – is required to obtain sufficient signal-to-noise.

### BASIC OPERATIONAL CONSTRAINTS

#### Beam Current

A satellite that can be approximated by a 2-m radius sphere has a capacitance  $C_{\text{sat}}$  of  $\sim 0.2$  nF. Neglecting charge neutralization processes, the satellite can emit approximately 10  $\mu\text{C}$  from a 50-kV beam source before the beam is emitted at zero voltage relative to infinity, or for approximately 50  $\mu\text{s}$  if a 200-mA beam (10 kW at 50 kV) is being generated. In contrast, given a beam voltage of 1 MV, the satellite can emit approximately 200  $\mu\text{C}$ , or a beam current of 10 mA for 20 ms.

Satellites are not isolated conductors; the orbital environment of most satellites is a neutral plasma, and charge neutralization will occur at some rate. That said, even without beam emission, spacecraft charging can be problematic from an operational standpoint [4,5]. There are several techniques for satellite charge neutralization, such as plasma contactors [6]; but in any case the satellite must eventually expel an equal but opposite charge as delivered by the electron beam. Thus, all else equal, for the same beam power a higher voltage beam provides an easier task for the neutralization system. This leads naturally to the selection of an RF-based accelerator.

#### High Voltage

The orbital environment of most satellites can be considered a neutral plasma. DC potentials will drive plasma currents and corresponding currents within the satellite [7,8]; high-voltage systems on satellites operating above approximately 30 kV have generally proven problematic and should be avoided if possible for the CONNEX mission [9]. This precludes very high-voltage DC guns, and also suggests that other systems requiring high voltages (such as most tube-based RF sources) are preferably avoided. HEMT RF amplifiers are typically driven with  $\sim 50$  V power supplies, addressing this concern.

#### Size, Weight and Power

Terrestrial accelerators are typically optimized based around the total cost of the installation, which for machines such as X-FELs tends to scale with the overall size of the facility. The typical approach is to increase the real-estate

\* Work supported by Los Alamos National Laboratory Pathfinder and Program Development. Approved for public release; distribution is unlimited; LA-UR-16-27164.

<sup>†</sup> jwlewellen@lanl.gov

gradient as much as practical by using high-shunt-impedance structures and using the highest-output RF sources available. Doing so increases the cost of the linac itself, but generally more slowly than the overall facility cost decreases (at least until significant technology development is required to meet real-estate gradient goals).

Satellite systems are highly constrained in overall size, weight and power consumption, and the tradeoffs are often encapsulated in the acronym SWaP: size, weight and power. While cost is always an area for consideration, it is on an equal rather than a dominant footing.

**Power and Energy Storage.** Power system constraints – including energy storage – represent one of the most significant limitations on a spaceborne accelerator. Specifically, the peak power draw of the linac will exceed the expected power output of the solar panels by approximately an order of magnitude; thus, power storage will be required, and both peak and average power draw must be considered.

The nominal 1 MeV, 10 mA beam draws 10 kW from the linac structure. Assuming the beam power is approximately equal to that dissipated in the structure, the linac will require 20 kW of RF power when beam is being generated. Assuming a nominal efficiency of 50% for the HEMT RF sources, the linac will require approximately 40 kW when generating beam.

The beam energy to be delivered per pulse for the CONEX experiment is 10 kJ; with a 10% HEMT duty cycle, the linac must operate for 10 s to deliver this integrated beam power. During this time the average power draw of the linac is 4 kW, and the total energy required is 40 kJ, or 11 W-hr. Figure 1 shows a comparison of the power density (W/kg) and energy storage density (W-hr/kg) of a number of battery types.

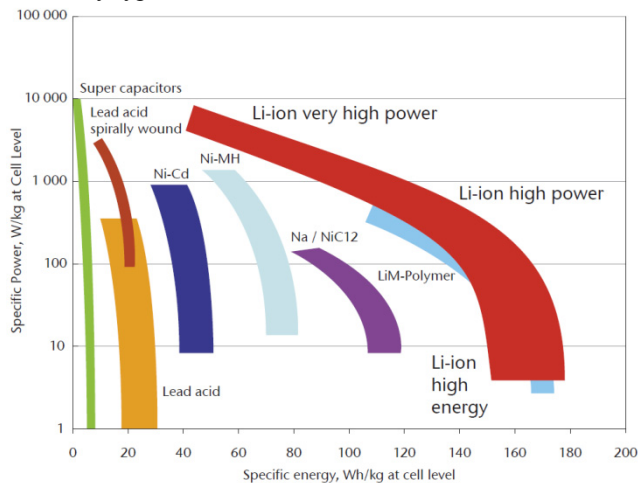


Figure 1: Specific power and energy density of various battery types. [10].

Very-high-power lithium-ion batteries are our notional downselect. While supercapacitors are appealing, few are space-qualified and they have a relatively low energy storage density. By fitting the battery bank with programmable interconnects, its cells can be connected in series to directly supply the ~50V required for the HEMTs, or in parallel for

recharging from the solar panels, with minimal additional power conversion.

**Temperature Stabilization.** Most terrestrial linacs are temperature-stabilized to keep the operating frequency constant. An active temperature-stabilization system represents a significant investment in SWaP for a spaceborne accelerator, and also a single point of failure. Our design concept eliminates active temperature stabilization, but rather tracks the operating frequency of the linac as its temperature changes. This approach is facilitated by the HEMT amplifier bandwidth of 15-20%, but for this technique to be viable for a multi-cell linac, all cells must change their frequency at the same rate, and our design reflects this requirement.

### Other Considerations

As intimated above, single-points-of-failure are to be avoided wherever possible in a satellite design. In the context of a satellite linac, eliminating a temperature stabilization system removes such a potential failure point; likewise, using a series of individual, low-power RF generators such as HEMTs offers the potential for increased fault tolerance vs. a single high-power RF source such as a klystron.

## LINAC DESIGN

The RF power required to drive a beam current  $I_b$  to a voltage  $V_b$  through a linac of length  $L$  is given by

$$P_{RF} = L \cdot \left( \frac{E_z^2}{R_s} + E_z I_b \right), \quad (1)$$

where  $E_z = \frac{V_b}{L}$  is the average accelerating field per unit length, also known as the real-estate gradient, and  $R_s$  is the shunt impedance per unit length. The first term in the equation is the power per unit length required to generate the desired average accelerating field; the second term is the power per unit length required to accelerate a beam at that field. RF-to-beam power efficiency can be increased by increasing the shunt impedance, increasing the beam current, or decreasing the average gradient while increasing the linac length to maintain a fixed voltage.

We selected ~5 GHz copper cavities (C-band) as a compromise between ease of fabrication, weight, and availability of RF power sources; a complementary but initially independent effort at SLAC selected X-band for similar reasons, and there appears to be a fairly broad optimum. SLAC have also performed a more general study considering other technologies as well, e.g. superconducting structures [11], but at this time normal-conducting structures in the C- to X-band appear the most promising for use on satellites.

Single- and few-cell RF guns that produce multi-MeV beams are quite common [12-14], but typically run at high gradients (50 – 100 MV/m) and, as they require several MW to operate, are infeasible for this application. Rather, we have designed a linac with a low on-axis accelerating field so as to reduce the first term in (1) while remaining within reasonable size limits.

### RF Structure Design and Power Source

An efficient re-entrant RF cavity, shown in Fig. 2, forms the basis for our linac design. Our nominal cavity has a gap corresponding to  $\beta = \frac{v}{c} = 0.2$  (approximately 10-keV electrons),  $Q_0 = 9000$ , and a resonant frequency of 5.1 GHz. Each cell requires approximately 170 W of RF power to deliver a maximum energy gain of 20 kV (corresponding to a peak on-axis field of 3 MV/m) for electrons with  $\beta \gg 0.2$ , for a net RF power requirement of 370 W per cell.

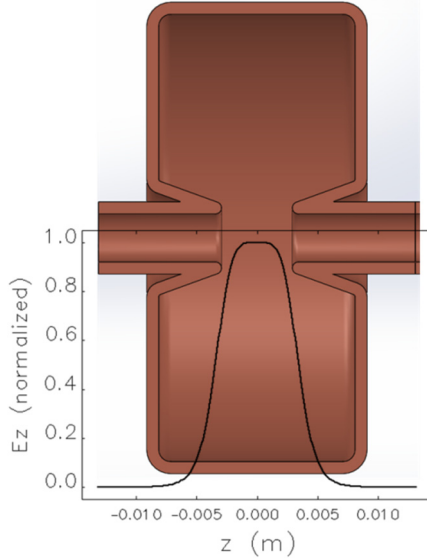


Figure 2: 5.1-GHz,  $\beta=0.2$  cavity and field profile.

The Wolfspeed CGHV59350 HEMT [15] has a nominal output power of up to 450 W, and efficiency of  $\sim 60\%$ . Thus, a single HEMT can power a single cavity in our notional linac design and is well-matched to the peak and average power draw estimates we made earlier. With an approximately 15% bandwidth, the HEMT can drive the cavity on-resonance as it swings through large temperature changes, given appropriate frequency feedback to the RF reference. These HEMTs can operate at up to 10% duty factor, with nominal pulse widths of 100  $\mu\text{s}$ . At LANL, we have successfully operated these HEMTs at lower power to 1 ms, and up to 800 W maximum output power.

As each cavity will have its own HEMT-based RF power source, it is reasonable to consider building local control electronics onto the same board holding the HEMT. Given the capabilities of FPGA-based systems, each cell can have its own suite of local controls and diagnostics, e.g. for reflected power monitoring and autophasing as described below. The use of a distributed low-level control system also helps increase overall system redundancy and robustness.

### Linac Design

With an injection energy of 10-20 keV, and a modest real-estate gradient of  $\sim 1$  MV/m, the beam's velocity increases relatively gradually along the linac, as shown in Fig. 3. Proton and ion accelerators address this situation with graded- $\beta$  designs, e.g. several different cell types, with gap lengths of  $\beta=0.2, 0.5$  and  $0.75$  for instance, along the linac to increase real estate gradient. In contrast, however, we

maintain the use of identical  $\beta=0.2$  cell throughout the linac, for three reasons.

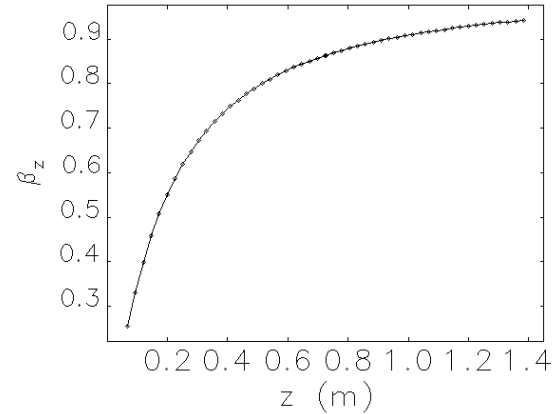


Figure 3: Beam velocity gain along the linac. Each dot represents the midpoint between two cavities.

First, all cells have nominally identical RF power dissipation and in principle corresponding temperature rise, greatly simplifying the frequency-tracking problem.

Second, each  $\beta=0.2$  cell can be powered by a single HEMT under normal operating conditions. Given the same shunt impedance, the larger gap of a higher- $\beta$  cell requires additional power both due to the additional wall losses and the higher voltage gain delivered to the beam. Multiple HEMTs per cell increases complexity and reduces commonality of operation across the linac.

Finally, while low- $\beta$  cells can effectively accelerate a high- $\beta$  beam, the reverse is not necessarily true. Using  $\beta=0.2$  cells along the linac allows ready operation at lower beam energy, either by intent (e.g. with increased beam current) or due to equipment malfunction (e.g. loss of acceleration in some cells due to HEMT failure). While the energy of a graded- $\beta$  linac can be lowered by shutting off downstream (higher- $\beta$ ) cells, the available range of beam currents will be lower. And, equipment failure in the lower- $\beta$  portions of the structure can cause a loss of acceleration efficiency in the higher- $\beta$  portions.

### Autophasing

To address multiple potential operating conditions (higher and lower voltage, component failure, etc.) we have developed a simple concept for automatic RF phase control.

Figure 4 illustrates the general concept. To set the phase of the RF field in the  $n^{\text{th}}$  cavity, pickups located between the cavities determine the arrival time of a bunch at the upstream and downstream ends of the  $n^{\text{th}}$  cavity, relative to the phase of the frequency reference; the average of the two times is a proxy for the beam's arrival time at the center of the cavity. The phase of the cavity field is then adjusted such that the on-axis field is at a maximum as the beam reaches the cavity's center.

By the time the beam has passed the 5<sup>th</sup> cavity (approximately 100 keV,  $\beta_{\text{beam}} \sim 0.55$ ), the fractional velocity change within each cell is small. For the initial cells, the approxi-

mation is good enough that no adjustment (e.g. cell-dependent phase shift) needs to be applied to the algorithm to obtain good results. However, implementing a desired phase shift on a cavity-by-cavity basis, for instance to improve beam capture, reduce energy spread or provide mild focusing, is a simple modification.

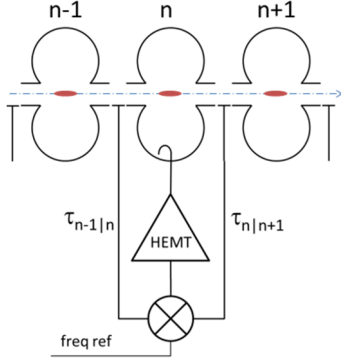


Figure 4: Satellite linac auto-phasing concept.

For an initial test of the concept, we generated a simulation of the 50-cell linac and a simplified 17-kV beam source with a short emission time, using Superfish [16] to calculate the fields and General Particle Tracer (GPT) [17] for the beam dynamics. GPT uses the convention

$$E_z(r, z) = E_z(z) \cos(\omega t + \phi) \quad (2)$$

so electrons receive maximum acceleration when  $\omega t + \phi = \pi$  when the beam is at the center of a cell.

The beam dynamics model is initially run with all cells' phases  $\phi_n$  set to a fixed initial phase; after each run, the new phase for each cavity is calculated by

$$\phi_n = \pi - \text{mod} \left( 2\pi f_0 \frac{\tau_{n-1|n} + \tau_{n|n+1}}{2}, 2\pi \right), \quad (3)$$

where  $\tau_{a|b}$  is the time the beam arrives at the pickup probe between cells  $a$  and  $b$ , and  $f_0$  is the cavity frequency of 5.1 GHz. The process is iterated until the beam energy at the end of the linac converges, as shown in Fig. 5. Note that since the process is based around local rather than global feedback, beam only has to transit the first cell at the first iteration, rather than the entire linac; once started, the algorithm generally converges to a solution in 10 – 15 iterations. The approach is fault-tolerant; Fig. 5 also shows the energy gain following “failures” (e.g. zero gradient) in 6 cells and rephasing (~5 iterations). With reasonable overhead in available HEMT power, the beam energy loss could easily be made up by slightly increasing the gradients in the remaining cells. The approach is also intrinsically adaptable to the inclusion of diagnostics, such as BPMs, along the linac.

### Beam Steering

Intra-linac steering correction will almost certainly be required; conventional steering correctors and feedback algorithms are mature and well-understood, and we do not foresee any significant difficulties in this area. Coarse steering of the beam as it exits the linac will be performed by orienting the satellite. Fine steering corrections can be

accomplished either with conventional electromagnets, or, if a very fast raster is desired, with transverse deflecting cavities.

### Frequency Control

The satellite linac concept, as described, utilizes only passive cooling. The use of identical cells will help to maintain all cells at the same resonant frequency (or within band), however, other factors such as beam loss will cause individual cells to have temperature changes somewhat different from the average across the linac.

The reflected power from the cavity is a good indication of frequency mismatch, providing the initial coupling and beam current are known; this allows each cavity's control electronics to determine whether it is above, below, or at the reference frequency. A global algorithm can adjust the RF power delivered to each cavity to raise or lower its temperature relative to the linac mean, while maintaining the final beam voltage.

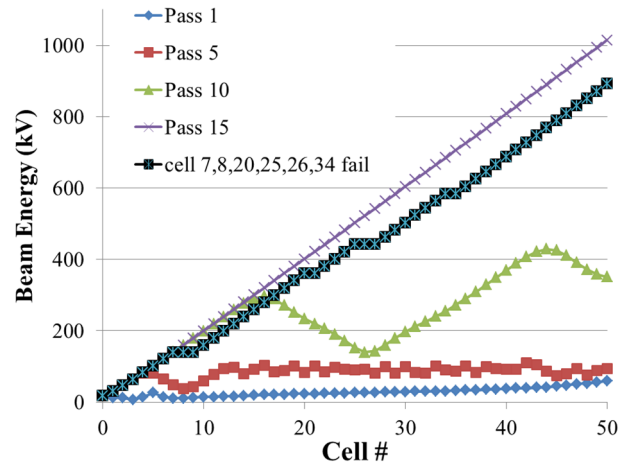


Figure 5: Beam energy after each cell in the linac, after 1, 5, 10 and 15 iterations of the autophasing algorithm, and after failure of multiple cells.

### Beam Source

There are several possible options for a beam source for the satellite linac. A relatively low-voltage DC gun, operating at 10 kV and with no bunching system, is the most straightforward option and represents the most mature technology choice; however, this reintroduces high-voltage DC also requires additional complexity in terms of cathode heater power supply isolation.

A small RF-based gun generating a beam at 15-20 kV would be the preferred option. While we do not have a final design yet, several concepts in the initial stages appear promising. For instance, a shorted-line cavity resonant at a subharmonic of the linac frequency can generate on-axis fields of several MV/m for ~300 W RF power consumption, and a thermionic cathode can supply the required beam current. Initial 1-d simulations show reasonable capture efficiency. The SLAC team is considering a “spark gap” gun making use of field-emission cathodes. [18]. In either case, an RF gun fitted with supplemental

HEMTs can provide improved reliability over a conventional DC gun.

## EXPERIMENTAL ACTIVITIES

While the basic physics underlying the satellite linac are relatively straightforward, the linac concept we propose requires the use of several unusual-for-accelerator technologies. To that end, LANL (and, independently, SLAC) initiated experimental programs to characterize HEMTs in the context of accelerator drivers, and explore related technologies.

We have tested C-band HEMTs up to 800 W for 2 ms into a load at low duty factors, with no faults or failures; from a single-pulse standpoint, the HEMTs perform considerably in excess of our requirements.

We have also used an HEMT to drive a test cavity based on the structure described above, up to the design gradient of 3 MV/m on-axis. Figure 6 shows a picture of the cavity under vacuum with no cooling as a start towards testing more and more faithful approximations of a spaceborne linac.

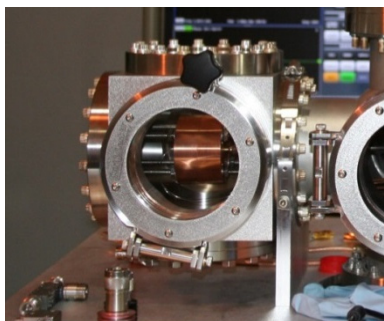


Figure 6: Test cavity in vacuum chamber.

The test cavity has a  $Q_0 \sim 5000$ , approximately half that of the nominal cavity design but with a similar interior geometry. As the cavity is set for unity coupling, little power is reflected, and the cavity reaches  $\sim 3$  MV/m peak on-axis fields at approximately 300 W from the HEMT. Thus, we can test both the HEMT's ability to source the required power for beam operations, concurrent with cavity and surface fields commensurate with that operation, without the presence of beam. In this configuration, the HEMT generated 500- $\mu$ s pulses at 5% duty factor, delivering an average power of 15 W to the cavity for several hours with no faults or vacuum excursions. As the HEMT is rated for sustaining a 5:1 VSWR without damage, this test was performed without a circulator between the HEMT output and the cavity.

## PATH FORWARD

To help build operational heritage for RF-based satellite linacs, we intend to propose an LCAS (low-cost access to space) sounding-rocket flight to test operation of a prototype spaceborne accelerator. The flight will be intended to not only build spaceflight heritage for the accelerator itself, but also explore beam-atmospheric interactions of scientific interest, and help validate CONNEX beam detection techniques.

To this end, LANL and SLAC have begun collaborating on the development of HEMT-driven linacs for satellite applications. Our next steps will be to downselect between C- and X-band. Follow-on work should include fabrication and assembly of a test beamline with several linac cavities and associated diagnostics. The line will initially facilitate measurement of beam energy gain (achievable gradient) and transverse focusing properties of the cavities using a 20-kV DC test beam. As gun concepts are developed, the line will also be used to prototype automatic frequency control and autophasing algorithms, and as a test platform for candidate beam sources.

## OTHER APPLICATIONS

An electron linac consisting of single cells, each driven by a powerful and compact solid-state amplifier, is a significant step forward in electron accelerator technology. This approach represents a paradigm shift from coupled-cell linacs driven by a single large high-power source, both in terms of the infrastructure requirements and in terms of fault tolerance and reliability. An HEMT-based MeV-range linac may be lighter and smaller overall than one driven by high-power RF tubes.

There are a number of applications in the terrestrial arena, such as radiography, medical waste sterilization, and medical applications, where such technology may be applicable. We welcome discussions regarding such potential applications.

## CONCLUSIONS

Advances in solid-state RF amplifier technology are facilitating new design paradigms for small, high-duty-factor electron linear accelerators intended for spaceborne applications, such as magnetosphere-ionosphere coupling studies. Such linacs may also be applicable to a wide variety of terrestrial applications.

## ACKNOWLEDGEMENTS

We wish to thank our colleagues at SLAC and at Goddard Space Flight Center for very fruitful and interesting discussions, and the CONNEX collaboration for their insight and support for this effort.

## REFERENCES

- [1] N. A. Tsyganenko, "Modeling the Earth's magnetospheric magnetic field confined within a realistic magnetopause," *J. Geophys. Res.*, vol. 100, no. A4, pp. 5599-5612, April 1995.
- [2] NASA, [http://ccmc.gsfc.nasa.gov/modelweb/models\\_home.html](http://ccmc.gsfc.nasa.gov/modelweb/models_home.html)
- [3] B. Abel and R.M. Thorne, "Electron scattering loss in Earth's inner magnetosphere: 1. Dominant physical processes," *J. Geophys. Res.*, vol. 103, no. A2, pp. 2385-2396, Feb. 1988.
- [4] J.F. Fennell, H.C. Koons, J.L. Roeder and J.B. Blake, "Spacecraft charging: observations and relationship to satellite anomalies," Aerospace Report No. TR-2001(8570)-5, August 2001.

- [5] T. Milaelian, "Spacecraft charging and hazards to electronics in space," <https://arxiv.org/pdf/0906.3884>, May 2001.
- [6] M.J. Patterson et al., "Plasma contactor development for space station," NASA Technical Memorandum 106425, 1993.
- [7] I. Katz, M. J. Mandell, G. W. Schnuelle, D. E. Parks, and P. G. Steen. "Plasma collection by high-voltage spacecraft at low earth orbit", J. Spacecraft and Rockets, vol. 18, No. 1 (1981), pp. 79-82.
- [8] S. Domitz and N.T. Grier, "The interaction of spacecraft high voltage power systems with the space plasma environment," Nasa Tech. Mem. NASA-TM-X-71554, 1974.
- [9] R. Friedel, LANL; private comm., 2016.
- [10] DOE Fact #607: "Energy and power by batter type," January 25, 2010.
- [11] E. Nanni, V. Dolgashev, S. Tantawi and J. Neilson, "COMPASS accelerator design technical overview," SLAC report SLAC-R-1058, January 2016.
- [12] J.W. Lewellen et al., "Operation of the APS RF gun," in Proc. XX Int'l Linear Accel. Conf., Chicago, Illinois, August. 1998.
- [13] S.G. Biedron et al., "The operation of the BNL/ATF Gun-IV photocathode RF gun at the Advanced Photon Source," in Proc. 1999 Part. Accel. Conf., New York, NY 1999.
- [14] J. Li et al., "Emission studies of photocathode RF gun at PITZ," in Proc of ICAP2012, Rostock-Warnemunde, Germany, 2012.
- [15] WolfSpeed preliminary data sheet: <http://www.wolfSpeed.com/downloads/dl/file/id/463/product/174/cghv59350.pdf>
- [16] J.H. Billen and L.M. Young, "Poisson Superfish," Los Alamos Technical Note LA-UR-96-1834, January 2006.
- [17] General Particle Tracer: <http://www.pulsar.nl/>
- [18] E. Nanni, SLAC; private comm. 2016.